LETTERS

Innate immune and chemically triggered oxidative stress modifies translational fidelity

Nir Netzer[1]*, Jeffrey M. Goodenbour[2]*, Alexandre David[1], Kimberly A. Dittmar[3], Richard B. Jones[4], Jeffrey R. Schneider[5], David Boone[5], Eva M. Eves[4], Marsha R. Rosner[4], James S. Gibbs[1], Alan Embry[1], Brian Dolan[1], Suman Das[1], Heather D. Hickman[1], Peter Berglund[1], Jack R. Bennink[1], Jonathan W. Yewdell[1]* & Tao Pan[3]*

Translational fidelity, essential for protein and cell function, requires accurate transfer RNA (tRNA) aminoacylation. Purified aminoacyl-tRNA synthetases exhibit a fidelity of one error per 10,000 to 100,000 couplings[1,2]. The accuracy of tRNA aminoacylation *in vivo* is uncertain, however, and might be considerably lower[3–6]. Here we show that in mammalian cells, approximately 1% of methionine (Met) residues used in protein synthesis are aminoacylated to non-methionyl-tRNAs. Remarkably, Met-misacylation increases up to tenfold upon exposing cells to live or non-infectious viruses, toll-like receptor ligands or chemically induced oxidative stress. Met is misacylated to specific non-methionyl-tRNA families, and these Met-misacylated tRNAs are used in translation. Met-misacylation is blocked by an inhibitor of cellular oxidases, implicating reactive oxygen species (ROS) as the misacylation trigger. Among six amino acids tested, tRNA misacylation occurs exclusively with Met. As Met residues are known to protect proteins against ROS-mediated damage[7], we propose that Met-misacylation functions adaptively to increase Met incorporation into proteins to protect cells against oxidative stress. In demonstrating an unexpected conditional aspect of decoding mRNA, our findings illustrate the importance of considering alternative iterations of the genetic code.

Owing to the central importance of tRNA aminoacylation and translational accuracy in understanding the biology of mammalian cells under normal and pathological conditions, we devised a method to measure tRNA misacylation in cells. Our method combines pulse radiolabelling of cells with [^{35}S]Met with microarrays developed for measuring tRNA abundance[8] (Fig. 1a and Supplementary Figs 1 and 2). We hybridized total tRNA to arrays that detect the 274 distinct chromosomal human tRNA species as closely related members of 42 families and all 22 mitochondrial tRNAs, and used phosphorimage analysis to visualize and quantify [^{35}S]Met-tRNAs hybridized to the array.

For HeLa cells, we detected intense radioactive spots representing five different methionyl-tRNA (tRNA^{Met}) probes, as expected. Unexpectedly, we easily detected less intense radioactive spots representing several non-tRNA^{Met} probes. Further, when we infected HeLa cells with influenza A virus or adenovirus 5 before pulse radiolabelling, the level of radioactive signals from non-tRNA^{Met} probes greatly increased (Fig. 1a), and could be exclusively detected by adding excess Met-oligonucleotide probes to block hybridization of tRNA^{Met} (Fig. 1b and Supplementary Fig. 3). We used multiple approaches to establish conclusively that radioactivity emanating from non-cognate tRNA probes derives from aminoacylated [^{35}S]Met and not other ^{35}S-containing material (detailed in Supplementary Methods and Supplementary Information). We excluded radiolabelling of tRNAs with thio-modifications by catabolism of [^{35}S]Met (Fig. 1c and Supplementary Fig. 4). We validated [^{35}S]Met-misacylation using two non-array-based methods for several tRNA species (Fig. 1d, e and Supplementary Fig. 5). To distinguish aminoacyl- from peptidyl-tRNAs, we treated total RNA with aminopeptidase M before array hybridization to remove amino (N)-terminal [^{35}S]Met residues from peptidyl-tRNAs (Fig. 1f and Supplementary Fig. 6). We also excluded misacylation resulting from contaminants in the [^{35}S]Met preparation (Supplementary Fig. 7).

In uninfected cells, the eight cytosolic misacylated tRNA families totalled approximately 1.5% of the cumulative radioactivity of all five tRNA^{Met} families. Upon infection with influenza A virus, misacylation increased in three of the eight species and appeared in 18 new tRNA families. Remarkably, the cumulative radioactivity on non-tRNA^{Met} species totalled about 13% of that of all tRNA^{Met} families (Fig. 1g and Supplementary Fig. 8). Cells infected with adenovirus or vaccinia virus demonstrated a similar pattern and degree of misacylation. Increased Met-misacylation in virus-infected cells is not an artefact of increased tRNA expression, because increased misacylation does not correlate with the minor changes in tRNA abundance induced by viral infection (Supplementary Fig. 9). Under all conditions tested, we failed to detect misacylation of any mitochondrial tRNA, demonstrating the selectivity of misacylation for cytosolic tRNAs (Fig. 1).

We next demonstrated tRNA-Met-misacylation *in vitro* (Supplementary Figs 10 and 11). HeLa-cell-derived methionyl-tRNA synthetase (MetRS) migrates in two major sucrose gradient fractions: one containing the 11-protein multi-synthetase complex, the other containing the multi-synthetase complex associated with polysomes[9]. Each sedimenting form of the multi-synthetase complex demonstrated similar acylation activity with [^{35}S]Met. The polysome-associated form clearly mediated misacylation among a subset of the misacylated tRNA families identified *in vivo*. The free form of the multi-synthetase complex exhibited less misacylation activity, demonstrating that the fidelity of tRNA synthetases can depend on the higher-order structure of the AARS. Further, we showed that although the multi-synthetase complex misacylated tRNA^{Lys} isoacceptors, free LysRS did not (Supplementary Fig. 11). This is consistent with misacylation being performed by MetRS within the multi-RS complex.

Because aminoacylated tRNAs can be used for non-translation functions[10,11], it was critical to establish whether Met-misacylated tRNAs are used in translation. A pulse-chase experiment revealed that cognate and non-cognate tRNAs demonstrate a similar off-rate for [^{35}S]Met after a 3-min chase period with excess unlabelled Met (Fig. 2a). Blocking translation by incubating cells with cycloheximide during

[1]Laboratory of Viral Diseases, National Institute of Allergy and Infectious Diseases, Bethesda, Maryland 20892, USA. [2]Department of Human Genetics, [3]Department of Biochemistry and Molecular Biology, [4]Ben May Institute, [5]Department of Medicine, University of Chicago, Chicago, Illinois 60637, USA.
*These authors contributed equally to this work.

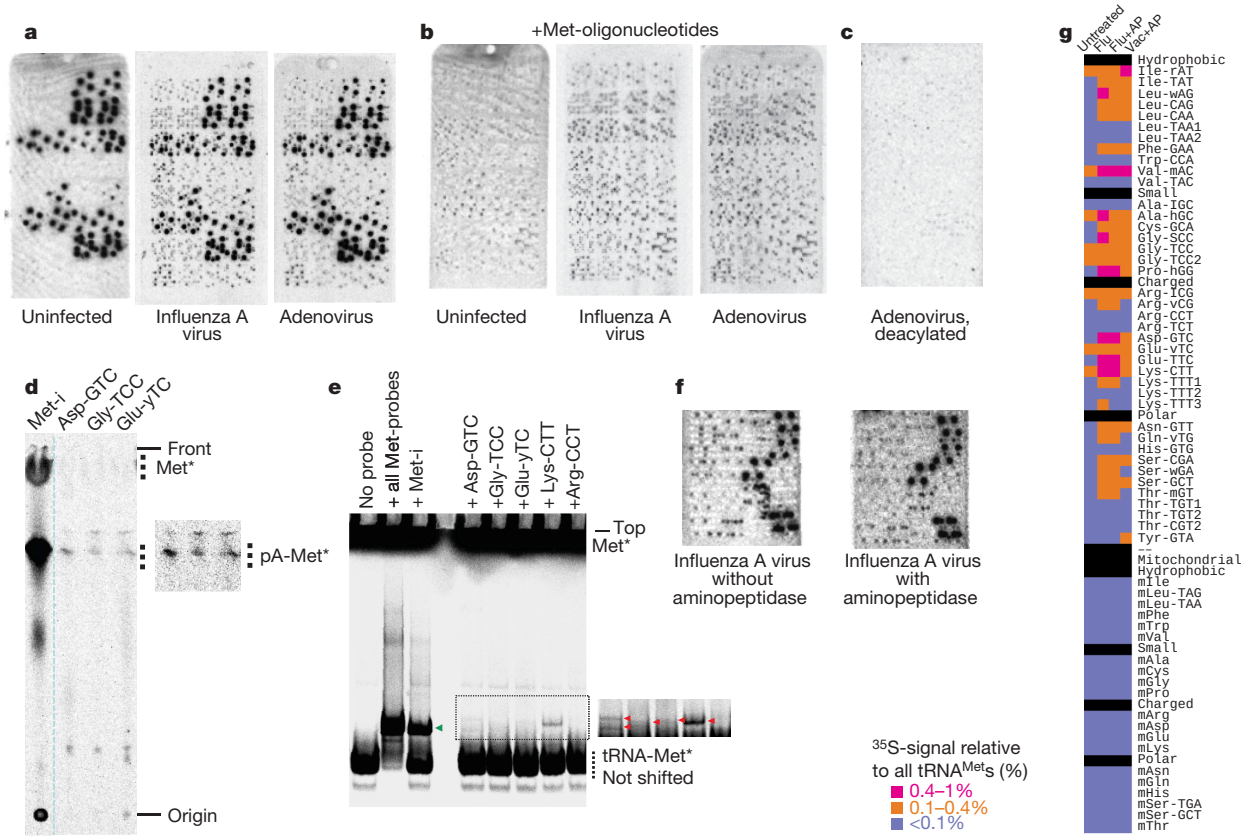

Figure 1 | Induction of tRNA misacylation by viruses. **a**, Microarrays showing total tRNAs isolated from uninfected, influenza A virus- and adenovirus-infected HeLa cells. **b**, Large excess of oligonucleotides complementary to $tRNA^{Met}$ was included in array hybridization. **c**, The adenovirus-infected sample was deacylated before array hybridization. **d**, Thin-layer chromatography of the influenza A virus-infected sample using biotinylated oligonucleotide probes (longer exposure in inset). **e**, Non-denaturing acid gel detection of misacylated tRNAs in the influenza A virus-infected sample. **f**, Influenza A virus-infected sample with or without aminopeptidase. **g**, Quantitative comparison of uninfected and virus-infected samples. tRNAs are grouped according to amino-acid properties. The detection limit of misacylation was about 0.1% for each probe.

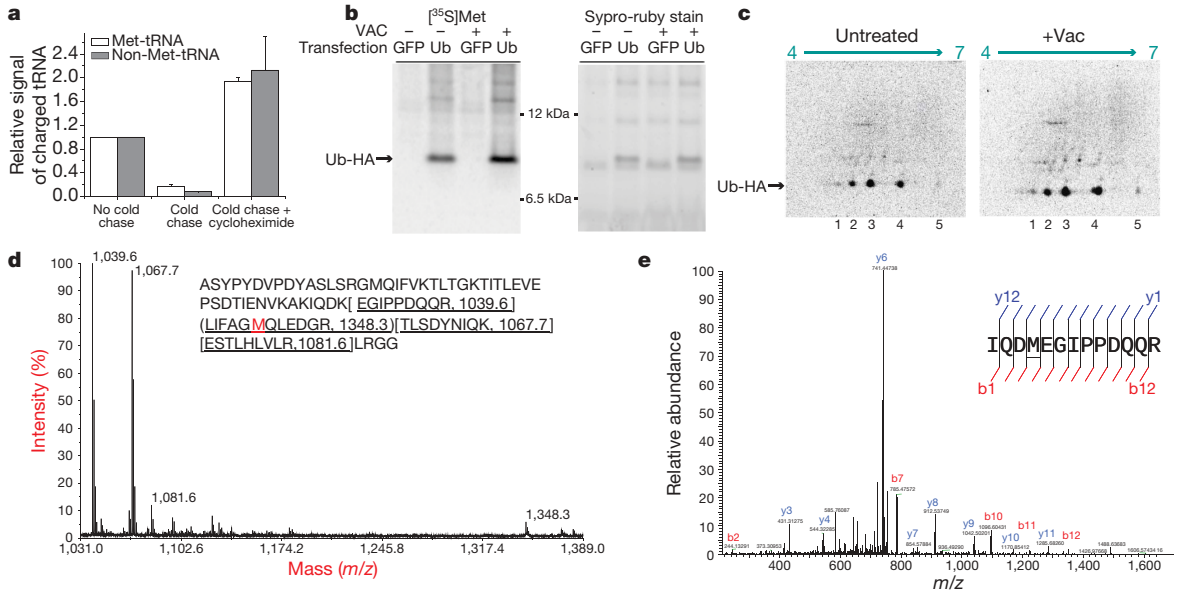

Figure 2 | Misacylated tRNAs are used in translation. **a**, Correctly acylated and misacylated tRNAs have the same kinetic properties with or without cycloheximide. Error bars represent s.d. ($n = 4$). **b**, One-dimensional SDS–polyacrylamide gel electrophoresis showing an increase in specific activity of [^{35}S]Met incorporation upon infection with vaccinia virus. **c**, Two-dimensional SDS–polyacrylamide gel electrophoresis of uninfected and vaccinia virus-infected samples. Spot 3 (55–62% of all radioactivity) matches the expected isoelectric point (pI) of wild-type Ub-HA. Spots 1 and 5 correspond to Lys/Arg-to-Met and Glu/Asp-to-Met substitution, respectively. **d**, Matrix-assisted laser desorption/ionization–time of flight of tryptic digested Ub-HA. Peaks are labelled with their m/z values from the Ub-HA sequence. **e**, Mass spectrometry–mass spectrometry sequencing of 763.87 ($m/2z$) mass peak by liquid chromatography–Fourier transform mass spectrometry (LC–FTMS) of tryptic digested Ub-HA.

the cold Met chase prevented the loss of [^{35}S]Met from cognate and non-cognate tRNAs in parallel (Fig. 2a and Supplementary Fig. 12a, b). These findings strongly support global use of misacylated tRNAs in protein synthesis. Next, we quantified the incorporation of [^{35}S]Met into haemagglutinin-epitope-tagged ubiquitin (Ub-HA), selected as a reporter because it possesses a single Met residue. Infecting cells with vaccinia virus increased the specific activity of Ub (dpm per μg protein) by about 1.8-fold, consistent with vaccinia-virus-induced increase in tRNA misacylation (Fig. 2b). Two-dimensional gel electrophoresis demonstrated vaccinia-virus-induced alterations consistent with translational use of misacylated tRNAs (Fig. 2c). Mass spectrometry detected Ub peptides containing Lys-to-Met substitutions, confirming the translation of misacylated tRNA^{Lys} (CTT) as predicted from the array data (Fig. 2d, e).

We detected virus-induced increases in misacylation (Supplementary Fig. 13) and global use of Met-misacylated tRNAs in protein synthesis (Supplementary Fig. 14) even when viral infectivity was inactivated by ultraviolet irradiation. Exposing HeLa cells, which express all human toll-like receptors (TLRs)[12], to the TLR3 ligand polyinosine-cytosine (poly-IC, which mimics double-stranded viral RNA), or the TLR4 ligand lipopolysaccharide (LPS, derived from bacterial cell walls) also increased tRNA misacylation (Fig. 3a and Supplementary Fig. 15a). LPS- and poly-IC-induced misacylation patterns overlapped significantly with each other and with virus-induced misacylation. We obtained similar results with CpG oligonucleotides, a TLR9 ligand (data not shown). Not all immune signalling events increase [^{35}S]Met-misacylation in HeLa cells, however. Exposing cells to interferon-β or interferon-γ did not increase misacylation, although each cytokine altered the expression of cytoplasmic and mitochondrial tRNAs within 24 h of initial exposure (data not shown).

We extended these findings to mouse bone-marrow-derived dendritic cells (Fig. 3b–d and Supplementary Fig. 15b), and liver cells in a living mouse by injecting [^{35}S]Met into the portal vein (Fig. 3e). Both cell types demonstrated a level and pattern of tRNA misacylation similar to HeLa cells, firmly establishing the *in vivo* relevance of misacylation. We failed to detect misacylation after labelling cells with either [^{35}S]Cys or ^{3}H-labelled Ile, Phe, Val or Tyr (Supplementary Fig. 16; note that specific activities of other commercially available amino acids are too low to detect misacylation at greater than 0.5%). Thus, misacylation could well be limited to Met.

As viral and bacterial infections activate myriad stress response pathways in cells, we examined the ability of chemical or physical stressors to modulate misacylation. We incubated HeLa cells at 42 °C, or exposed them to the Asn-linked glycosylation inhibitor tunicamycin or the proteasome inhibitor MG132, treatments that induce an unfolded protein response through distinct pathways[13]. Although tunicamycin and MG132 increased tRNA misacylation by approximately twofold, heat shock decreased tRNA misacylation by approximately twofold (Supplementary Fig. 17). The pattern of misacylation induced by tunicamycin and MG132 was limited to subset of RNA families seen in response to viruses and TLR ligands. Allowing HeLa cells to grow past confluence, a condition known to induce stress-related genes[14], also induced misacylation (Supplementary Fig. 16b).

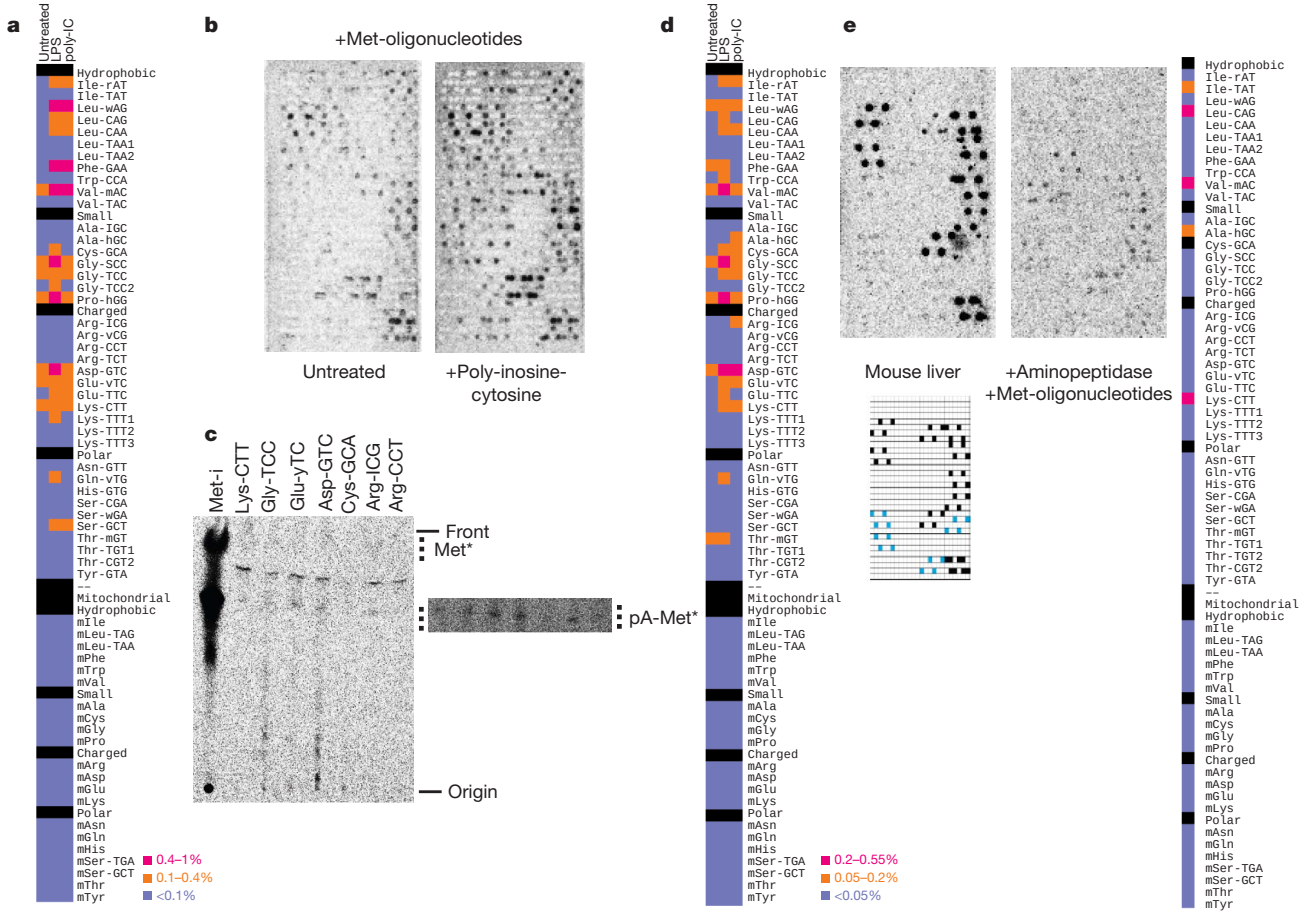

Figure 3 | tRNA misacylation induced by TLR ligands. **a**, Comparison of untreated and LPS, poly-IC-treated HeLa samples. **b**, Comparison of immature and poly-IC-matured bone marrow dentritic cells including complementary Met-oligonucleotides in array hybridization. **c**, Thin-layer chromatography of the poly-IC-matured sample using biotinylated probes. **d**, Quantitative comparison of untreated, LPS and poly-IC-matured dendritic cell samples, all aminopeptidase-treated. The detection limit of tRNA misacylation for these samples was about 0.05% for each probe. **e**, Misacylation occurs *in vivo*. Misacylation for total charged tRNA isolated from mouse liver after a 1-min pulse with [^{35}S]Met. Array key shows probe locations for Met-tRNAs (black) and Cys-tRNAs (blue).

Heightened generation of ROS by activation of NADPH oxidases is a common downstream effect of many cellular stressors[13]. It is well established that genetically encoded Met residues can act in *cis* to protect enzyme active sites against ROS-mediated damage[15], and Met protects *Escherichia coli* against oxidative-damage-induced death[7]. ROS oxidize the highly reactive sulphur in Met, which is restored to its reduced state by Met-sulphoxide reductases through NADPH oxidation[16]. We hypothesized that tRNA Met-misacylation protects cells against oxidative stress by replacing the amino acids we identified in the arrays with Met. Because tRNA misacylation is induced rapidly, this mechanism allows immediate extra-genetic incorporation of Met residues in newly synthesized proteins that provide protection against increased ROS levels.

As predicted by this hypothesis, exposing HeLa cells to ROS-inducing agents (arsenite, telluride or H_2O_2) induces Met-misacylation at high levels (Fig. 4a, b and Supplementary Fig. 18a, b). Arsenite-induced misacylation did not require protein synthesis, as it was unaffected by the addition of cycloheximide at the time of arsenite exposure (Supplementary Fig. 12c). Oxidizing agents act at least in part by increasing cellular NADPH oxidase activity[17], and in each case, misacylation was significantly reduced by diphenyleneiodonium (DPI), a broad inhibitor of these oxidases. TLR activation is known to induce ROS in neutrophils and dendritic cells[18]. Remarkably, treating HeLa cells with DPI inhibited poly-IC-induced misacylation, implicating ROS as the trigger for TLR-induced misacylation (Fig. 4b, c and Supplementary Fig. 18c). DPI also inhibited LPS and poly-IC-induced misacylation in dendritic cells (Fig. 4d, e).

We propose that Met-misacylation is a protective response to cellular stressors that increase levels of ROS. This is consistent with the recent proposal that the ROS scavenging capacity of Met selects for mitochondrial genetic recoding of AUA from Ile to Met[19]. Alternative explanations for Met-misacylation include the possibilities that it is a non-productive by-product of oxidative stress that exacerbates stress by decreasing translational fidelity (particularly because replacement of charged surface residues with Met would be predicted to increase protein aggregation), and that misacylated Met tRNAs function in cellular methylation or amino-acid transport pathways[20].

It has been demonstrated that upon mutating aminoacyl-tRNA synthetases or introducing exogenous misacylating tRNAs, *E. coli*, yeast and mice tolerate and adapt to increased errors in tRNA aminoacylation[3,21,22]. Theoretical considerations[23] support higher error thresholds for translational fidelity than those observed for tRNA aminoacylation *in vitro*. We demonstrate that mammalian cells have an intrinsic ability to modify tRNA misacylation and translational fidelity. The extent to which this ability, currently limited to Met, extends to any of the 14 amino acids yet to be examined, is an open question.

In summary, we have shown that tRNA misacylation with Met is a common and regulated event in mammalian cells. Although the full

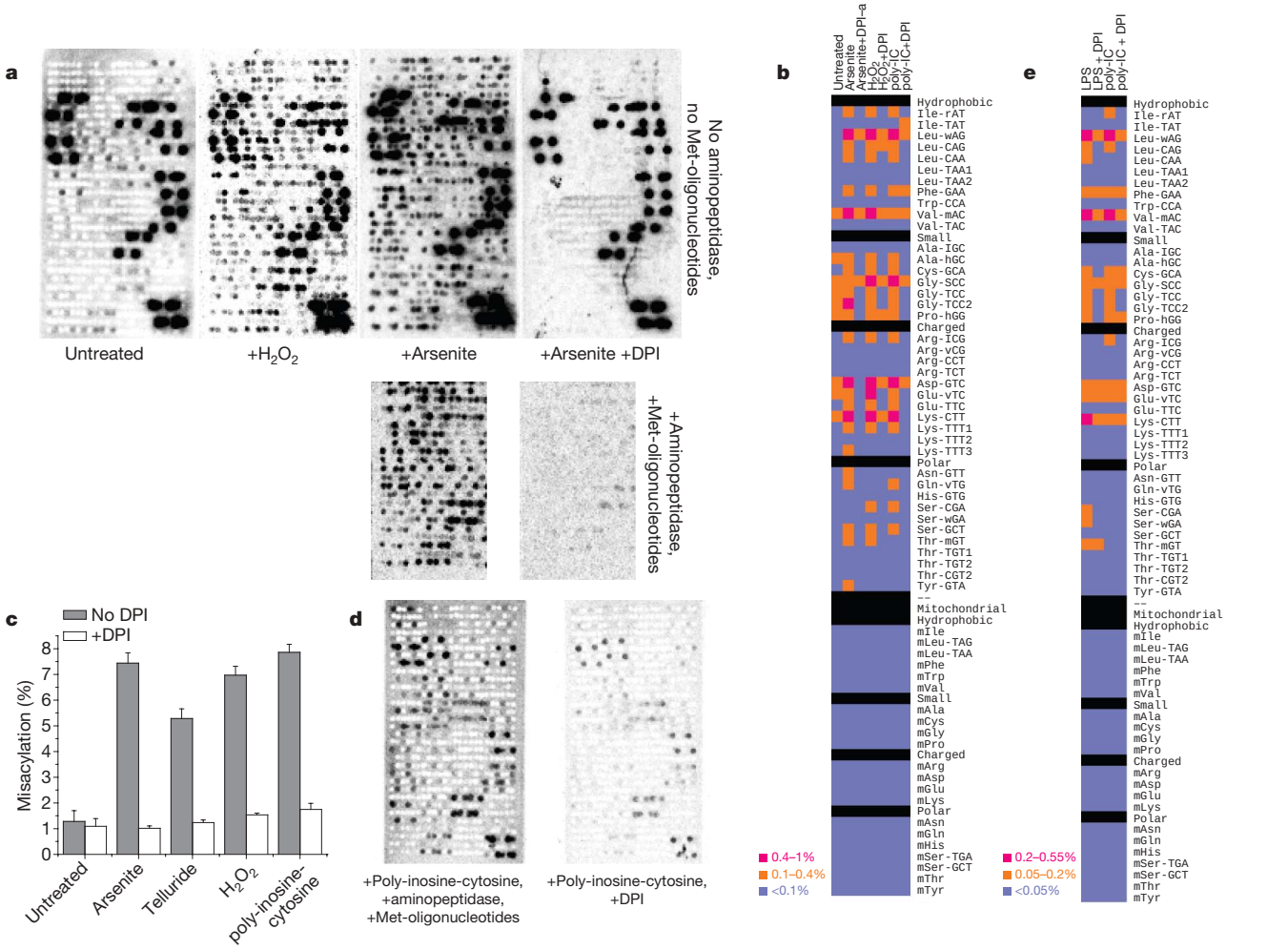

Figure 4 | Oxidative stress induces NADPH-oxidase-dependent RNA misacylation. **a**, tRNA misacylation in HeLa cells induced by oxidizing agents H_2O_2 (1 h) or arsenite (4 h). DPI inhibits arsenite-induced misacylation. **b**, Quantitative comparison of tRNA misacylation under oxidative stresses (arsenite and H_2O_2) and TLR ligand (poly-IC) with or without DPI. **c**, Percentage of all misacylated tRNAs with or without DPI when cells were treated under four conditions (100% = all Met-tRNAs). Error bars represent s.d. ($n = 2$). **d**, Poly-IC induces NADPH-oxidase-dependent tRNA misacylation in dendritic cells. **e**, Quantitative comparison of tRNA misacylation in dendritic cells with or without DPI.

implications of this phenomenon remain to be explored, there is a practical consequence: decoding mRNA into protein in living cells is not as simple as generally believed. tRNA-misacylation-based protein sequence diversity, like RNA splicing and post-translational modifications, may represent an evolutionary strategy for expanding and manipulating the information encoded by nucleic acids[24].

METHODS SUMMARY

The Methods section includes cell growth, cell treatment and stress conditions, misacylation *in vivo*, immune-precipitation of Ub-HA, two-dimensional polyacrylamide gel electrophoresis and mass spectrometry, detection of tRNA misacylation by TLC and native acid gels, pH 9 deacylation, nuclease treatment of arrays, *in vitro* aminoacylation and acylated tRNA extraction for microarrays.

Microarray. The basic features of the tRNA microarray have been described previously to determine tissue-specific differences in human tRNA expression[8]. Both array versions contain about 50 probes (42 unique) for chromosomal human and mouse tRNAs, 22 probes for human mitochondrial tRNAs and 18 probes for mouse mitochondrial tRNAs. The first array version contains 20 repeats for each probe, and over 50 hybridization control probes for tRNAs from bacteria, yeast, *Drosophila* and *Caenorhabditis elegans*. The second array version contains eight repeats for each probe and six hybridization controls for tRNAs from bacteria and yeast. The second version contains fewer repeats per probe but has higher sensitivity due to improved array printing techniques. Both versions contain four probes for chromosomal initiator and elongator $tRNA^{Met}$ and one for mitochondrial $tRNA^{Met}$.

Array hybridization was performed on a Genomic Solutions Hyb4 station with 10 μg total RNA in 2 × SSC, pH 4.8 at 60 °C for 50 min. This short hybridization time was the same as the half-life of [^{35}S]Met-labelled aminoacylated tRNAs (Supplementary Fig. 19) and was necessary to minimize the amount of hydrolysis of aminoacylated tRNA during hybridization. After hybridization, arrays were washed twice each, first in 2 × SSC, pH 4.8, 0.1% SDS, then in 0.1 × SSC, pH 4.8, spun dry and exposed to phosphorimaging plates (Fuji Medicals) for up to 14 (^{35}S labels) or 34 days (^{3}H labels using ^{3}H plates). Spot intensity was quantified using Fuji Imager software.

Received 26 August; accepted 9 October 2009.

1. Ibba, M. & Soll, D. Aminoacyl-tRNA synthesis. *Annu. Rev. Biochem.* **69,** 617–650 (2000).
2. Cochella, L. & Green, R. Fidelity in protein synthesis. *Curr. Biol.* **15,** R536–R540 (2005).
3. Lee, J. W. *et al.* Editing-defective tRNA synthetase causes protein misfolding and neurodegeneration. *Nature* **443,** 50–55 (2006).
4. Miranda, I., Silva, R. & Santos, M. A. Evolution of the genetic code in yeasts. *Yeast* **23,** 203–213 (2006).
5. Silva, R. M. *et al.* Critical roles for a genetic code alteration in the evolution of the genus *Candida*. *EMBO J.* **26,** 4555–4565 (2007).
6. Ahel, I., Korencic, D., Ibba, M. & Soll, D. Trans-editing of mischarged tRNAs. *Proc. Natl Acad. Sci. USA* **100,** 15422–15427 (2003).
7. Luo, S. & Levine, R. L. Methionine in proteins defends against oxidative stress. *FASEB J.* **23,** 464–472 (2009).
8. Dittmar, K. A., Goodenbour, J. M. & Pan, T. Tissue-specific differences in human transfer RNA expression. *PLoS Genet.* **2,** e221 (2006).
9. Ussery, M. A., Tanaka, W. K. & Hardesty, B. Subcellular distribution of aminoacyl-tRNA synthetases in various eukaryotic cells. *Eur. J. Biochem.* **72,** 491–500 (1977).
10. Varshavsky, A. Regulated protein degradation. *Trends Biochem. Sci.* **30,** 283–286 (2005).
11. Ibba, M. & Soll, D. Quality control mechanisms during translation. *Science* **286,** 1893–1897 (1999).
12. Nishimura, M. & Naito, S. Tissue-specific mRNA expression profiles of human toll-like receptors and related genes. *Biol. Pharm. Bull.* **28,** 886–892 (2005).
13. Malhotra, J. D. *et al.* Antioxidants reduce endoplasmic reticulum stress and improve protein secretion. *Proc. Natl Acad. Sci. USA* **105,** 18525–18530 (2008).
14. Murray, J. I. *et al.* Diverse and specific gene expression responses to stresses in cultured human cells. *Mol. Biol. Cell* **15,** 2361–2374 (2004).
15. Levine, R. L., Mosoni, L., Berlett, B. S. & Stadtman, E. R. Methionine residues as endogenous antioxidants in proteins. *Proc. Natl Acad. Sci. USA* **93,** 15036–15040 (1996).
16. Oien, D. B. & Moskovitz, J. Substrates of the methionine sulfoxide reductase system and their physiological relevance. *Curr. Top. Dev. Biol.* **80,** 93–133 (2008).
17. Chernyak, B. V. e. t. a. l. Production of reactive oxygen species in mitochondria of HeLa cells under oxidative stress. *Biochim. Biophys. Acta Bioenergetics* **1757,** 525–534 (2006).
18. Savina, A. *et al.* NOX2 controls phagosomal pH to regulate antigen processing during crosspresentation by dendritic cells. *Cell* **126,** 205–218 (2006).
19. Bender, A., Hajieva, P. & Moosmann, B. Adaptive antioxidant methionine accumulation in respiratory chain complexes explains the use of a deviant genetic code in mitochondria. *Proc. Natl Acad. Sci. USA* **105,** 16496–16501 (2008).
20. Finkelstein, J. D. Metabolic regulatory properties of *S*-adenosylmethionine and *S*-adenosylhomocysteine. *Clin. Chem. Lab. Med.* **45,** 1694–1699 (2007).
21. Ruan, B. *et al.* Quality control despite mistranslation caused by an ambiguous genetic code. *Proc. Natl Acad. Sci. USA* **105,** 16502–16507 (2008).
22. Santos, M. A., Cheesman, C., Costa, V., Moradas-Ferreira, P. & Tuite, M. F. Selective advantages created by codon ambiguity allowed for the evolution of an alternative genetic code in *Candida* spp. *Mol. Microbiol.* **31,** 937–947 (1999).
23. Hoffmann, G. W. On the origin of the genetic code and the stability of the translation apparatus. *J. Mol. Biol.* **86,** 349–362 (1974).
24. Freist, W., Sternbach, H., Pardowitz, I. & Cramer, F. Accuracy of protein biosynthesis: quasi-species nature of proteins and possibility of error catastrophes. *J. Theor. Biol.* **193,** 19–38 (1998).

Supplementary Information is linked to the online version of the paper at www.nature.com/nature.

Acknowledgements The authors are grateful to D. Klinman for his gift of CpG oligonucleotides and advice, A. Schilling for supervision and advice on mass spectrometry experiments, and C. Nicchitta, T. Pierson, P. Cluzel, R. Levine, A. Iwasaki and S. Amigorena for insight and advice. This work was supported by the Division of Intramural Research, the National Institute of Allergy and Infectious Diseases, and by National Institutes of Health extramural pilot projects.

Author Contributions N.N., J.M.G., A.D., K.A.D., R.B.J., J.R.S., D.B., E.M.E, M.R.R., J.S.B., A.E., B.D., S.D., H.D.H., P.B. and T.P. designed and performed experiments, and analysed data. J.S.G. generated genetic constructs. J.R.B. and J.W.Y designed experiments and analysed data. J.W.Y. and T.P. conceived the project and wrote the paper. J.W.Y. and T.P. contributed equally to this paper.

Author Information The microarray platforms are deposited in the National Center for Biotechnology Information (NCBI) Gene Expression Omnibus (GEO) database under accession numbers GPL9427 and GPL9428. Reprints and permissions information is available at www.nature.com/reprints. Correspondence and requests for materials should be addressed to J.W.Y. (jyewdell@nih.gov) or T.P. (taopan@uchicago.edu).